



MATHEMATICAL MODELING OF MHD FLOW OF HYBRID MICROPOLAR FERROFLUIDS ABOUT A SOLID SPHERE

Hamzeh T. Alkawasbeh *

Department of Mathematics, Faculty of Science, Ajloun National University, Ajloun 26810, Jordan

ABSTRACT

The purpose of this study is mathematical simulation the combined free convection of hybrid micropolar ferrofluids about a solid sphere with magnetic force. We studied the magnetic oxide (Fe_3O_4) and Cobalt Iron Oxide (CoFe_2O_4) nanoparticles and suspended them into water–ethylene glycol (EG) ($\text{H}_2\text{O}+(\text{CH}_2\text{OH})_2$) (50-50%) mixture. Numerical results for correlated physical quantities were gained through the Keller Box method along with the assistance of MATLAB software. The influence of relevant contributing parameters on physical quantities are inspected through tables and graphical illustrations. According to the current findings, the mono ferrofluid has the highest local skin friction, heat transmission rate, velocity and angular velocity profiles. Moreover, it has the lowest temperature.

Keywords: Hybrid Micropolar Ferrofluids; Solid Sphere; MHD; Free Convection.

1. INTRODUCTION

Nanofluids have a plethora of applications in electronics cooling, power production, nuclear energy, solar energy collectors, agriculture, geophysics, and industrial processes, among others (Saeedi et al. (2018), Toghraie et al. (2020) Sahim et al (2021)). Over the last two decades, nanofluids have been extensively studied and shown to have superior thermal characteristics compared to conventional liquids and air (Mahian et al. (2021) and Ahmadi et al. (2018)). By extension, Ferrofluids are a kind of nanofluid in which magnetic nanoparticles such as iron, nickel, and cobalt are suspended in a base fluid to create a colloidal system. Their physical characteristics and flow field vary adaptively in response to external magnetic field characteristics Kandelousi (2017), which enables them to be used in a variety of applications (Alkawasbeh et al. (2020) and Mohamed et al. (2021)) especially, medical applications such as drug targeting, cell separation, and magnetic resonance imaging Patra et al. (2018). Numerous studies have been conducted in this field Wang and Wang (2014).

To better understand the effects of magnetic fields on ferrofluid flow, Moghadam et al. Moghadam et al. (2021) looked at the flow of the ferrofluid inside a wavy duct with a variety of different parameters. When it came to friction coefficient and pressure loss, they found that magnetic number and wave amplitude had the most influence on improving Nu, while volume fraction and Reynolds number had the poorest effects. Ajith et al. (2021) carried out an experimental study to investigate the thermophysical properties of low-density MgFe_2O_4 ferrofluid synthesized with novel disk-shaped in the presence of magnetic forces. The study results reveal that through the attendance of 350 G magnetic field at 0.20 % volume fraction of magnesium ferrite nanoparticles, the thermal conductivity, the viscosity, and the density of ferrofluid rises by 13.92 %, 28.31 %, and 5.33 %, respectively. Hosseinizadeh et al. (2021) evaluated the energy and exergy performance of a triple tube heat exchanger employing ferrofluid under the impact of an external magnetic field. Zheng et al. (2021) researched the pressure loss and thermal efficiency of a plate heat exchanger using

ferrofluids in a variety of magnetic field configurations. The results indicate that a vertical placement of two magnets next to one another outside the sidewalls results in a 21.8 percent increase in average Nusselt number and a 10% decrease in average pressure drop when compared to no magnetic field scenarios. Abadeh et al. (2020) investigated the heat transfer rate and pressure drop of a ferrofluid in laminar flow in a circular straight tube under the influence of constant and alternate magnetic fields. Constant magnetic fields of 770 and 1300 G increased the Nu number by 9.43 and 11.96 percent, respectively. Additionally, it is claimed that by employing an alternate magnetic field with a frequency of 10 or 100 Hz, the Nu number is increased by 11.85 and 14.8%, respectively. It is also reported that increments in frequency (above 100 Hz to 1000 Hz) have no beneficial effect. Mehrez and El Cafsi (2021) quantitatively investigated heat exchange and Fe_3O_4 /water nanofluid flow characteristics in a horizontal rectangular tube exposed to the influence of a magnetic field. It is seen from the findings that a recirculation area is formed around the magnetic source, where the thermal boundary layer is eliminated, thus increasing local heat exchange. When the combined impacts of Fe_3O_4 nanoparticles and magnetic field are evaluated, the total heat exchange may reach up to 86 percent. The magnetohydrodynamic flow of ferrofluid in a channel with non-symmetric cavities was studied by Hussain et al. (2020) they reported that the most critical element to maximize the heat transfer is the geometry, namely the aspect ratio of the cavities. Using the Darcy–Forchheimer model, Tadesse et al. (2021). studied the heat transfer in hydrodynamic stagnation point flow of magnetite Fe_3O_4 /water nanofluid towards a convectively heated permeable sheet computationally, taking into account the effects of viscous dissipation, suction/injection, convective heating, and a magnetic field.

Nowadays, the employment of two distinct types of magnetic nanoparticles in the base fluid has grown increasingly popular, and it is termed hybrid ferrofluid. The right selection of nanoparticle combination and appropriate dispersion of the ferrofluid have a significant effect on the heat transfer rate increase (Gui et al. (2018, Abadeh et al. (2019), Saikrishnan et al (2021), Kole and Khandekar (2021)). Giwa et al. (2021) used the artificial neural network and the

* Corresponding author: hamzahtahak@yahoo.com

adaptive neuro-fuzzy inference system to determine the impact of various parameters on the thermophysical properties of hybrid Fe₂O₃-Al₂O₃ (75:25) ferrofluids. In the following study Giwa et al. (2020), they investigated the natural convection heat transmission of this hybrid ferrofluid loaded within a rectangular cavity and subjected to magnetic forces. According to their findings, the optimal heat transfer increase of 10.79 percent was obtained for a 0.10 volume fraction, and an additional enhancement of 4.91 percent was obtained by vertically inducing a magnetic field (118.4 G) on the cavity's sidewall. Tili et al. (2020) considered the impact of asymmetrical heat rise/fall on the MHD flow of hybrid ferrofluid. According to their results, suspending magnetic oxide and cobalt iron oxide in a 50–50 combination of H₂O and EG (ethylene glycol) significantly lowers the heat transfer rate under certain circumstances. Kumar et al. (2020) investigated the radiative thin film flow of water–ethylene glycol-based (Fe₃O₄/CoFe₂O₄) hybrid ferrofluid under the influence of irregular heat source/sink. Hosseinzadeh et al. (2020) analyzed micropolar MHD hybrid ferrofluid flow moving over a vertical plate, taking into account free convection heat transfer and magnetic field and for three distinct base fluids for the ferrofluid. Chu et al. (2020) discussed the hybridization of Fe₃O₄ and MWCNT inside a tank containing viscous fluid and porous medium under the influence of magnetism. The findings indicate that heat transport along walls improves when the Rayleigh and Darcy factors are used, but degrades when the magnetic field parameter is included.

It is widely established that the rheology of different ferrofluids deviates significantly from that of Newtonian fluid (García and Galindo (2020), Karvelas et al. (2020), and Li et al. (2020)). Thus, in order to represent the distinct differences in transport processes in ferrofluids, researchers use a variety of models, one of which is the micropolar model, which is defined by the micromotion of stiff, randomly oriented (or spherical) particles floating in a viscous medium. Afzal et al. (2021) evaluated the thermo-radiation, magnetic field, as well as uniform heat source impacts on stream and heat transmission of nanofluid across an extending surface, using micropolar and Carreau models. Waqas et al. (2021) examined the bioconvection movement of a micropolar nanofluid over a fine needle using a thermal and an exponential space-based heat source. It is concluded from the findings that increasing the Biot number as well as thermal radiation improves the thermal dispersal. The concentration of nanoparticles drops as the Brownian motion parameter increases but increases with the thermophoresis parameter. In a similar study by Khan et al. (2021a), the same type of flow over a moving needle was subjected to binary chemical reaction viscous dissipation and Arrhenius activation energy. Thermal profile increases with increasing Eckert number, thermophoretic, volumetric fraction, and Brownian motion parameter values, according to their findings. Concentration profiles diminish when Lewis number, thermophoretic parameter, chemical reaction, and Brownian motion parameter values increase, but improve as activation energy parameter values rise. El-dawy and Gorla (2021) investigated the influence of heat generation/absorption and an applied magnetic field on the flow of a micropolar nanofluid across a stretching and contracting wedge. Khan et al. (2021b) addressed the non-Newtonian behavior of micropolar nanofluid cross-diffusion flow in terms of heat generation/absorption and the effects of radiative heat flux. Habib et al. (2021a) showed the impact of thermal radiations and magnetic forces on the mass and heat transfer of a micropolar nanofluid through bio-convection across a permeable stretched sheet. Al-Khaled et al. (2021) theoretically analyzed the impact of non-uniform heat source/sink on the bioconvection-radiative flow of nanofluid with microorganisms using Brinkman micropolar model. The results demonstrated that tilting and Brinkman factors decrease nanofluid velocity, while non-uniform heat source/sink parameters and Brinkman parameters increase their temperature. Habib et al. (2021b) carried out a comparative study of nanofluids flow owing to a stretching sheet using various non-Newtonian models such as micropolar, Williamson, and Maxwell model in the presence of double diffusion, activation energy, and

bioconvection. Ramesh et al. (2021) incorporated injection/suction and slip effects on Time-dependent motion study of Casson-micropolar nanofluid confined between two parallel disks with the upper one is squeezing the nanofluid flow by moving along the axial direction.

By the best of authors' knowledge, the current literature does not give a substantial contribution to the analysis of flow and heat transfer in the micropolar hybrid ferrofluids model. Considering the importance of MHD on improving the heat transfer rate it seems that the subject is of great value. Also, the literature review shows that the MHD on micropolar hybrid ferrofluids flow with free convection has not been considered yet. Here, the problem of free convection flow of water containing hybrid ferrofluids about a sphere within the MHD field is studied. In next section, after the explaining the problem and the governing equations, the numerical procedure is explained. The results are discussed using the temperature profile, heat transfer coefficient, heat flux and friction factor diagrams and finally at last section the conclusion is presented.

2. MATHEMATICAL MODEL

Suppose we have a (water-ethylene glycol) 50% flow containing suspensions of (CoFe₂O₄, Fe₃O₄) nanoparticles in the presence of combined convection around a solid sphere of radius a under the impact of Lorentz force along with constant wall temperature T_w , in addition to a surrounding temperature T_∞ are taken into consideration. Fig 1 displays the flow layout and the schematic diagram, where g stands for heat gravity vector. Here \hat{x} -coordinate is measured along the circumference of the sphere at the stagnation point ($\hat{x}=0$), while the \hat{y} -coordinates is perpendicular to the sphere surface.

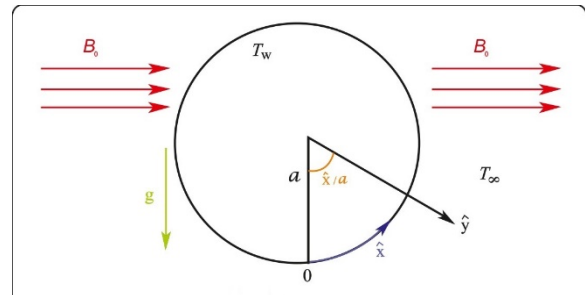


Fig. 1 Layout and geometrical coordinates flow

The continuity equation is derived from the law of mass conservation, which states that the mass does not change during its motion, while the momentum equation describes the movement of viscous fluids. it was constructed by Claude-Louis Navier and George Gabriel Stokes by applying Newton's second law, this equation later became known as the Navier-Stokes equation. Besides, the thermal energy equation displays the conservation of energy for a fluid element. it was derived by employing the first law of thermodynamics. However, the equations of continuity, momentum, and thermal energy for the steady-state flow of viscous incompressible fluid so the governing system of micropolar hybrid ferrofluid modeling can be written as

$$\frac{\partial}{\partial \hat{x}}(\hat{r}\hat{u}) + \frac{\partial}{\partial \hat{y}}(\hat{r}\hat{v}) = 0, \quad (1)$$

$$\rho_{hff} \left(\hat{u} \frac{\partial \hat{u}}{\partial \hat{x}} + \hat{v} \frac{\partial \hat{u}}{\partial \hat{y}} \right) = (\mu_{hff} + \kappa_0) \frac{\partial^2 \hat{u}}{\partial \hat{y}^2} + \beta_{hff} g (T - T_\infty) \sin\left(\frac{\hat{x}}{a}\right) + \kappa_0 \frac{\partial \hat{H}}{\partial \hat{y}} - \sigma_{hff} B_0^2 \hat{u}, \quad (2)$$

$$\hat{u} \frac{\partial T}{\partial \hat{x}} + \hat{v} \frac{\partial T}{\partial \hat{y}} = \alpha_{hff} \frac{\partial^2 T}{\partial \hat{y}^2}, \quad (3)$$

$$\rho_{hff} \Gamma \left(\hat{u} \frac{\partial \hat{H}}{\partial \hat{x}} + \hat{v} \frac{\partial \hat{H}}{\partial \hat{y}} \right) = \gamma_{hff} \frac{\partial^2 \hat{H}}{\partial \hat{y}^2} - \kappa_0 \left(2\hat{H} + \frac{\partial \hat{u}}{\partial \hat{y}} \right), \quad (4)$$

with boundary conditions defined as (Alkaskasbeh (2018), and Swalmeh et al. (2018))

$$\hat{u} = \hat{v} = 0, T = T_w, \hat{H} = -\frac{1}{2} \frac{\partial \hat{u}}{\partial \hat{y}} \text{ as } \hat{y} = 0$$

$$\hat{u} \rightarrow 0, T \rightarrow T_\infty, \hat{H} \rightarrow 0 \text{ as } \hat{y} \rightarrow \infty, \quad (5)$$

where $\Gamma = a^2/\sqrt{Gr}$ is micro-inertia density.

All other symbols and quantities are given in nomenclature of the hybrid ferrofluid. β_{hff} , ρ_{hff} , μ_{hff} , α_{hff} , $(\rho c_p)_{hff}$, k_{hff} , and σ_{hff} are coefficient of thermal expansion, density, viscosity thermal diffusivity, heat capacity, thermal conductivity and electrical conductivity of hybrid ferrofluid, which are defined by as

$$\beta_{hff} = (1 - \chi_2) \left[(1 - \chi_1) \beta_f + \chi_1 \beta_{s1} \right] + \chi_2 \beta_{s2}$$

$$\rho_{hff} = (1 - \chi_2) \left[(1 - \chi_1) \rho_f + \chi_1 \rho_{s1} \right] + \chi_2 \rho_{s2},$$

$$\mu_{hff} = \frac{\mu_f}{(1 - \chi_1)^{2.5} (1 - \chi_2)^{2.5}},$$

$$(\rho c_p)_{hff} = (1 - \chi_2) \left[(1 - \chi_1) (\rho c_p)_f + \chi_1 (\rho c_p)_{s1} \right] + \chi_2 (\rho c_p)_{s2},$$

$$\frac{k_{hff}}{k_{bf}} = \frac{(k_{s2} + 2k_{bf}) - 2\chi_2 (k_{bf} - k_{s2})}{(k_{s2} + 2k_{bf}) + \chi_2 (k_{bf} - k_{s2})},$$

where $\frac{k_{bf}}{k_f} = \frac{(k_{s1} + 2k_f) - 2\chi_1 (k_f - k_{s1})}{(k_{s1} + 2k_f) + \chi_1 (k_f - k_{s1})},$ (6)

$$\alpha_{hff} = \frac{k_{hff}}{(\rho c_p)_{hff}},$$

$$\frac{\sigma_{hff}}{\sigma_f} = 1 + \frac{3 \left[\frac{\chi_1 \sigma_1 + \chi_2 \sigma_2}{\sigma_f} - (\chi_1 + \chi_2) \right]}{\left[\frac{\chi_1 \sigma_1 + \chi_2 \sigma_2}{\sigma_f} + 2 \right] - \left[\frac{\chi_1 \sigma_1 + \chi_2 \sigma_2}{\sigma_f} - (\chi_1 + \chi_2) \right]}$$

The non-dimensional variables defined as (Alkaskasbeh (2018))

$$\hat{x} = ax, \hat{y} = aGr^{-1/4}y, \hat{r} = ar, \hat{u} = \left(\frac{v_f}{a} \right) Gr^{1/2}u, \hat{v} = \left(\frac{v_f}{a} \right) Gr^{1/4}v,$$

$$\hat{H} = \left(\frac{v_f}{a^2} \right) Gr^{3/4}H, (T - T_\infty) = \theta(T_w - T_\infty), \quad (7)$$

The Grashof number defined as $Gr = (g\beta_f(T_w - T_\infty)a^3)/\nu_f^2$, $\hat{r}(\hat{x}) = a \sin(\hat{x}/a)$ is the radial distance from the symmetric axis to the sphere surface and $\gamma_{hff} = (\mu_{hff} + \kappa_0/2)\Gamma$ is spin gradient of hybrid ferrofluid

Substituting equations (6) and (7) into equations (1) to (4), we get the non-dimensional equations

$$\frac{\partial}{\partial x}(ru) + \frac{\partial}{\partial y}(rv) = 0, \quad (8)$$

$$u \frac{\partial u}{\partial x} + v \frac{\partial u}{\partial y} = \frac{\rho_f}{\rho_{nf}} (D_1 + K) \frac{\partial^2 u}{\partial y^2} + \frac{1}{\rho_{hff}} D_2 \theta \sin x$$

$$+ \frac{\rho_f}{\rho_{hff}} K \frac{\partial H}{\partial y} - \frac{\rho_f}{\rho_{hff}} \frac{\sigma_{hff}}{\rho_f} Mu,$$

$$(9)$$

$$u \frac{\partial \theta}{\partial x} + v \frac{\partial \theta}{\partial y} = \frac{1}{Pr} D_3 \frac{\partial^2 \theta}{\partial y^2}, \quad (10)$$

$$u \frac{\partial H}{\partial x} + v \frac{\partial H}{\partial y} = -\frac{\rho_f}{\rho_{hff}} K \left(2H + \frac{\partial u}{\partial y} \right) + \frac{\rho_f}{\rho_{hff}} \left(D_1 + \frac{K}{2} \right) \frac{\partial^2 H}{\partial y^2}, \quad (11)$$

where

$$D_1 = \frac{1}{(1 - \chi_1)^{2.5} (1 - \chi_2)^{2.5}},$$

$$D_2 = (1 - \chi_2) \left[\chi_1 (\rho_{s1} \beta_{s1} / \beta_f) + (1 - \chi_1) \rho_f \right] + \chi_2 (\rho_{s2} \beta_{s2} / \beta_f),$$

$$D_3 = \frac{k_{hff} / k_f}{(1 - \chi_2) \left[(1 - \chi_1) \rho_f + \chi_1 (\rho c_p)_{s1} / (\rho c_p)_f \right] + \chi_2 (\rho c_p)_{s2} / (\rho c_p)_f},$$

$Pr = \nu_f / \alpha_f$ is the Prandtl number,

$$M = \left(\frac{\sigma_f B_0^2 a^2 Gr^{-1/2}}{\rho_f \nu_f} \right) \text{ is the magnetic parameter and}$$

$K = (\kappa_0 / \mu_f)$ is micro-rotation parameter.

The boundary conditions (5) become to

$$u = v = 0, \theta = 1, H = -\frac{1}{2} \frac{\partial u}{\partial y} \text{ at } y = 0, \quad (12)$$

$$u \rightarrow 0, \theta \rightarrow 1, H \rightarrow 0, \text{ as } y \rightarrow \infty.$$

To solve the non-dimensional equations (8) to (11), with boundary conditions (12), we use the following transformation variables

$$\varpi = xr(x)f(x,y), \theta = \theta(x,y), H = xh(x,y), \quad (13)$$

where ϖ is the stream function defined as

$$(ru) = \varpi_y \text{ and } (rv) = -\varpi_x, \quad (14)$$

Thus equations (9) to (11) in dimensionless form assume the following become

$$\frac{\rho_f}{\rho_{hff}} (D_1 + K) \frac{\partial^3 f}{\partial y^3} + (1 + x \cot x) f \frac{\partial^2 f}{\partial y^2} - \left(\frac{\partial f}{\partial y} \right)^2 + \frac{1}{\rho_{hff}} D_2 \frac{\sin x}{x} \theta$$

$$+ \frac{\rho_f}{\rho_{hff}} K \frac{\partial h}{\partial y} - \frac{\rho_f}{\rho_{hff}} \frac{\sigma_{hff}}{\rho_f} M \frac{\partial f}{\partial y} = x \left(\frac{\partial f}{\partial y} \frac{\partial^2 f}{\partial x \partial y} - \frac{\partial f}{\partial x} \frac{\partial^2 f}{\partial y^2} \right), \quad (15)$$

$$\frac{D_3}{Pr} \frac{\partial^2 \theta}{\partial y^2} + f \frac{\partial \theta}{\partial y} (1 + x \cot x) = x \left(\frac{\partial f}{\partial y} \frac{\partial \theta}{\partial x} - \frac{\partial f}{\partial x} \frac{\partial \theta}{\partial y} \right), \quad (16)$$

$$\frac{\rho_f}{\rho_{nf}} \left(D_1 + \frac{K}{2} \right) \frac{\partial^2 h}{\partial y^2} + (1 + x \cot x) f \frac{\partial h}{\partial y} - \frac{\partial f}{\partial y} h$$

$$- \frac{\rho_f}{\rho_{nf}} K \left(2h + \frac{\partial^2 f}{\partial y^2} \right) = x \left(\frac{\partial f}{\partial y} \frac{\partial h}{\partial x} - \frac{\partial f}{\partial x} \frac{\partial h}{\partial y} \right), \quad (17)$$

The boundary conditions are reduced to

$$f = \frac{\partial f}{\partial y} = 0, \theta = 1, h = -\frac{1}{2} \frac{\partial^2 f}{\partial y^2} \text{ at } y = 0,$$

$$\frac{\partial f}{\partial y} \rightarrow 0, \theta \rightarrow 0, h \rightarrow 0 \text{ as } y \rightarrow \infty. \quad (18)$$

The local skin friction coefficient Cf and the Nusselt number Nu which are interest in this problem can be expressions as

$$Cf = \frac{a^2}{Gr^{3/4} \mu_f \nu_f} \tau_w, Nu = \frac{a}{k_f (T_w - T_\infty)} q_w, \quad (19)$$

where

$$\tau_w = \left(\mu_{hff} + \frac{\kappa_0}{2} \right) \left(\frac{\partial \hat{u}}{\partial \hat{y}} \right)_{\hat{y}=0}, q_w = -k_{hff} \left(\frac{\partial T}{\partial \hat{y}} \right)_{\hat{y}=0}. \quad (20)$$

Using the transformations described above then the Cf and Nu written as

$$Cf = Gr^{-1/4} \left(D_1 + \frac{K}{2} \right) x \frac{\partial^2 f}{\partial y^2}(x, 0), \quad Nu = -Gr^{1/4} \frac{k_{hff}}{k_f} \left(\frac{\partial \theta}{\partial y} \right)(x, 0). \quad (21)$$

3. NUMERICAL SOLUTION

A technique called the Keller box technique was introduced by Keller and Bramble (1970) in 1970. This method became popular when Jones Jones (1981) used it to solve boundary layer-related problems. Cebeci and Bradshaw (2012) provided an extensive explanation of this method in their book.

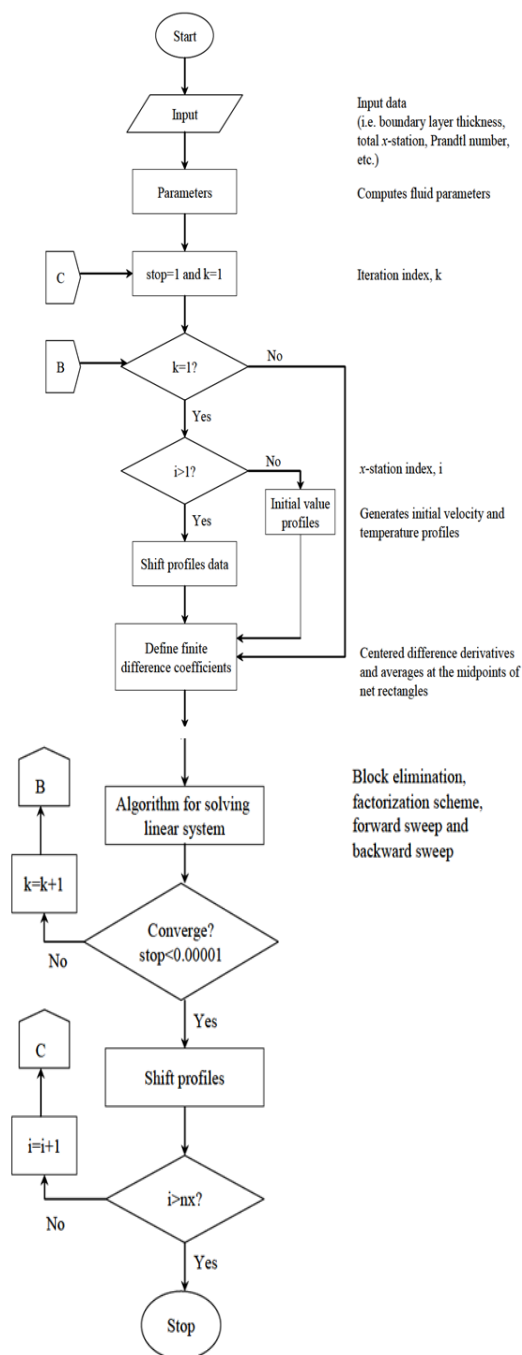


Fig. 2: Flowchart the Keller box method

The Keller-box method was employed in the current study to construct a numerical solution for the problem. At the beginning of this method, the transformed governing equations are reformulated to obtained first-

order equations. Next, the central differences technique is employed to find the difference equations. Then, Newton's procedure is used to linearize the obtained equations. After that, the matrix-vector form is written. Finally, the tridiagonal matrix is obtained and the linear system is solved via LU decomposition. The MATLAB program has been used to perform numerical calculations considering the wall shear stress as a convergence criterion, which is often employed in laminar boundary layer computations to achieve the required accuracy. This is most likely due to the fact that the wall shear stress in the laminar boundary layer calculations has the maximum error (see Cebeci and Bradshaw (2012)). Therefore, the numerical schemes were repeated until the convergence criterion was satisfied, in which the numerical findings obtained were accurate to six decimal places. The solution is obtained by the Flowchart are illustrated in Figure 2.

4. RESULTS AND DISCUSSIONS

In this section, numerical computations were implemented via MATLAB to obtain graphical and numerical results for the flow characteristics of (water-ethylene glycol) 50% as a host micropolar hybrid ferrofluid in the presence of the effects of some pertinent parameters as well as provide a thorough parametric analysis. In such an analysis, the numerical results are observed when a single examine parameter varies over the range, whereas other examine parameters remain constant. It is a typical analysis usually used by mathematicians, physicists, and engineers in modelling and decision making. The parameters that were taken into account in the calculations are micro-rotation K , magnetic M , and nanoparticle volume fraction χ_1, χ_2 and have ranges of $K > 0, M > 0$ and $0.1 \leq \chi_i \leq 0.2$, where $i = 1, 2$.

Table 1. show the thermo-physical properties of (water-ethylene glycol) 50% and the ultrafine particles that were employed in this work. In order to verification the accuracy current numerical results, they were compared with prior results published in previous literature, see Tables 2 and 3

Table 1 Thermo-physical properties of nanoparticles.(Esfahani et al. (2017))

	$\rho(kg\ m^{-3})$	$C_p(J\ kg^{-1}\ K^{-1})$	$k(W\ m^{-1}\ K^{-1})$	$\beta \times 10^{-5}(K^{-1})$	$\sigma(S\ m^{-1})$
(H ₂ O+EG)50%	1056	3288	0.425	0.00341	0.00509
(Fe ₃ O ₄)	5180	670	9.7	20.6	0.74×10^6
(CoFe ₂ O ₄)	4907	700	3.7	27.4	1.1×10^7
Pr	29.86				

Table 2 Comparison of Nu for different values x at $Pr = 7, M = K = 0$, and $\chi_1 = \chi_2 = 0$

x degree	Huang and Chen (1987) $\times 10^{-4}$	Swalmeh et al. (2018) $\times 10^{-6}$	Present $\times 10^{-6}$
0	9581	958212	958213
10	9559	956150	956151
20	9496	949791	949793
30	9389	939133	939132
40	9239	924124	924122
50	9045	904676	904675
60	8858	880677	880678
70	8518	851943	851942
80	8182	818819	818818
90	7792	779807	779805
100	-	733822	733824
110	-	682876	682874
120	-	624790	624792

Table 3 Comparison of Cf for different values x at $Pr = 7$,
 $M=K=0$ and $\chi_1 = \chi_2 = 0$

x degree	Huang and Chen (1987) $\times 10^{-4}$	Swalmeh et al. (2018) $\times 10^{-6}$	Present $\times 10^{-6}$
0	0	0	0
10	876	87746	87742
20	1737	173925	173924
30	2566	256914	256915
40	3350	335445	335444
50	4075	407947	407948
60	4727	472964	472967
70	5293	529422	529424
80	5762	577331	577330
90	6123	612909	612907
100	-	637137	637138
110	-	645776	645774
120	-	644746	644745

Figures 3 and 4 confirmed that local Nusselt number and local skin friction are decreasing functions of the magnetic parameter. Actually, this reduction is caused by curbing that occurs in the fluid movement induced by the rise in the intensity of the magnetic field that restrains convection, hence reducing it. physically, the heightening in the strength of the magnetic field product a force kind which called Lorentz force, where the results in convinced facing to the fluid flow particles consequently, restraint the fluid flow.

Figures 5 and 6 are related to the impact of micro-rotation parameter on local Nusselt number and local skin friction, it can be observed the positive effect of the micro-rotation parameter on skin friction and its negative effect on Nusselt number. This is expected because the micro-rotation parameter reduces the local skin friction factor and local Nusselt number. Moreover, the aforementioned figures confirmed that simple nanofluid $(Fe_3O_4)/(H_2O+EG)$ is superior in terms of Cf and Nu , regardless of the value of variables parameters M or K , when comparison with micropolar hybrid ferrofluid $(CoFe_2O_4+Fe_3O_4)/(H_2O+EG)$

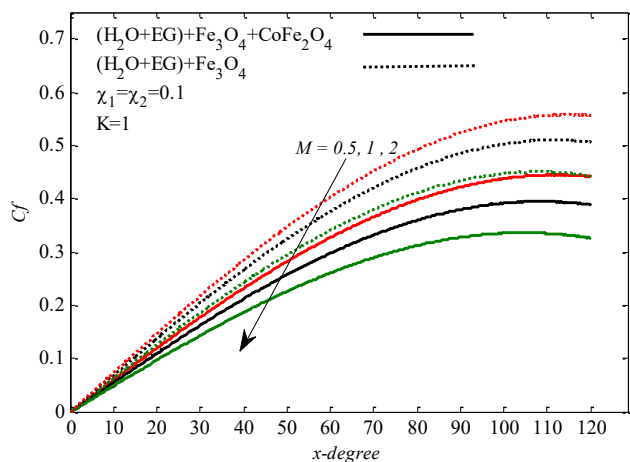


Fig. 3 Changes in Cf due to variation in M

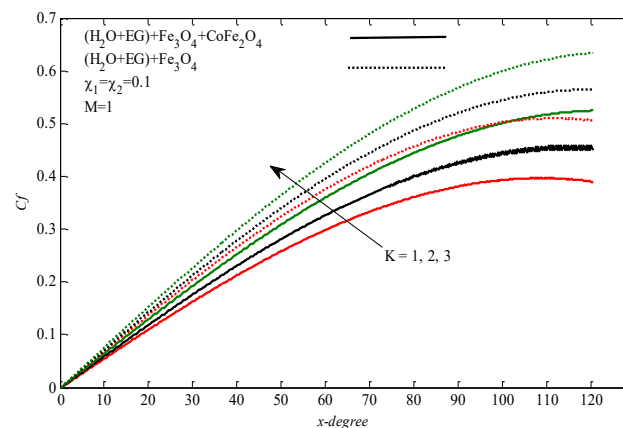


Fig. 5 Changes in Cf due to variation in K

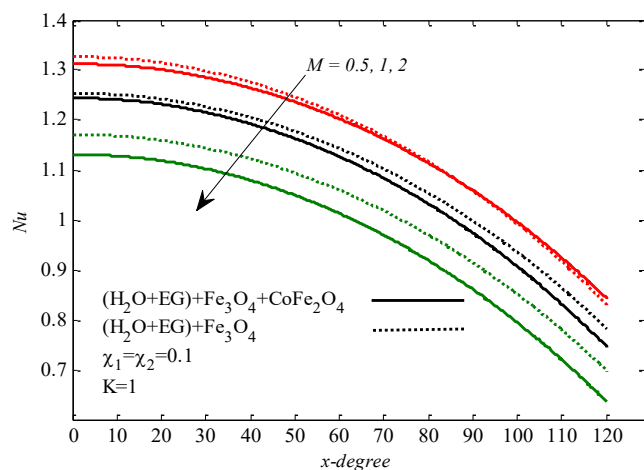


Fig. 4 Changes in Nu due to variation in M

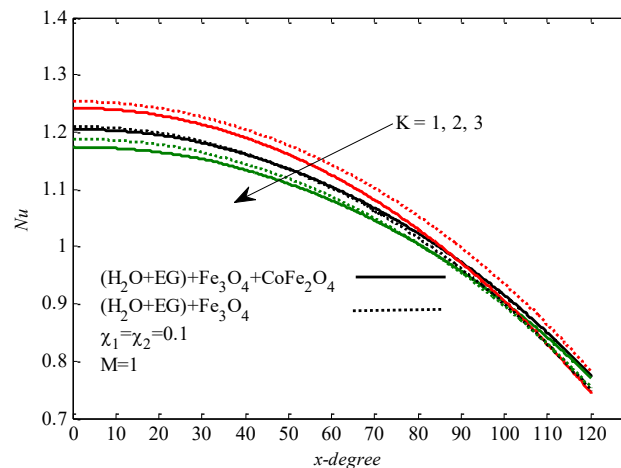


Fig. 6 Changes in Nu due to variation in K

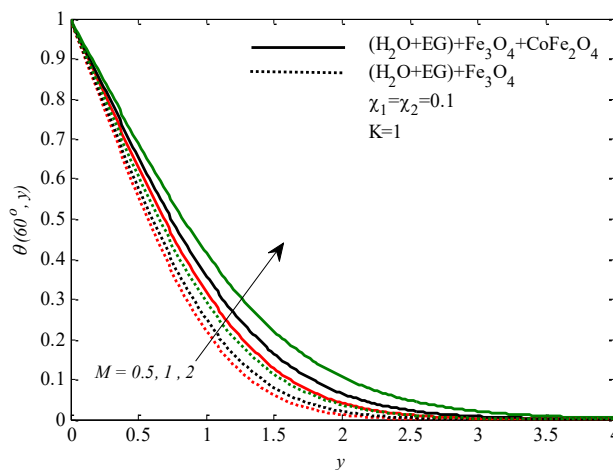


Fig. 7 Changes in θ due to variation in M

Figures 7-9 illustrate the effect of magnetic parameter, velocity and angular velocity at $x = 60^\circ$, respectively, the temperature rises but the velocity and angular velocity are reduces. Of course, this will happen because crossing a magnetic field through a moving fluid generates a force called the Lorentz force, which, as a result, boosts the resistance of the hybrid ferrofluid to motion. We also noticed that hybrid ferrofluid gained the highest temperature for the values of the magnetic parameters affecting it. But for velocity and angular velocity turns out to us the mono ferrofluid are highest

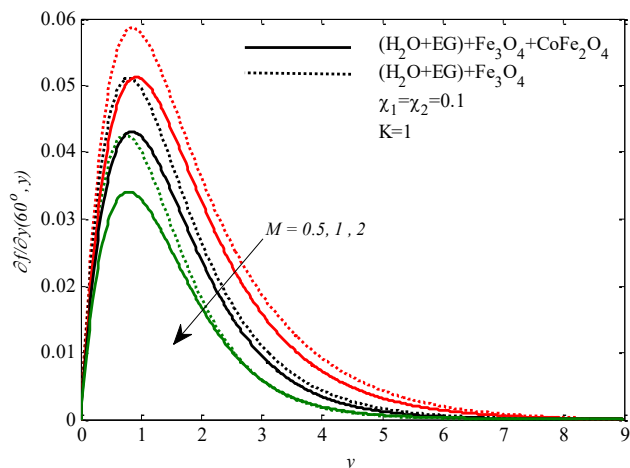


Fig. 8 Changes in $\partial f/\partial y$ due to variation in M

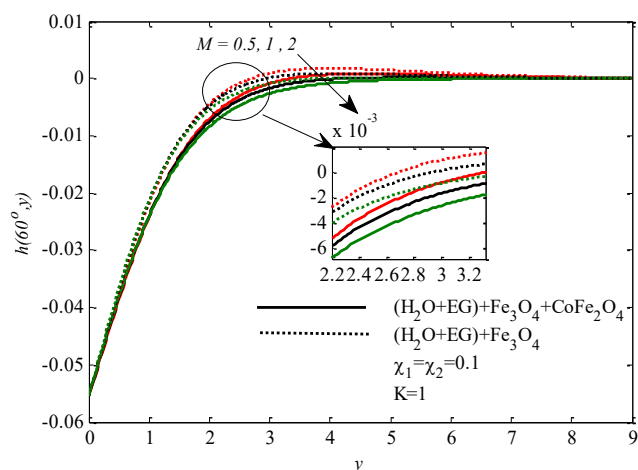


Fig. 9 Changes in h due to variation in M

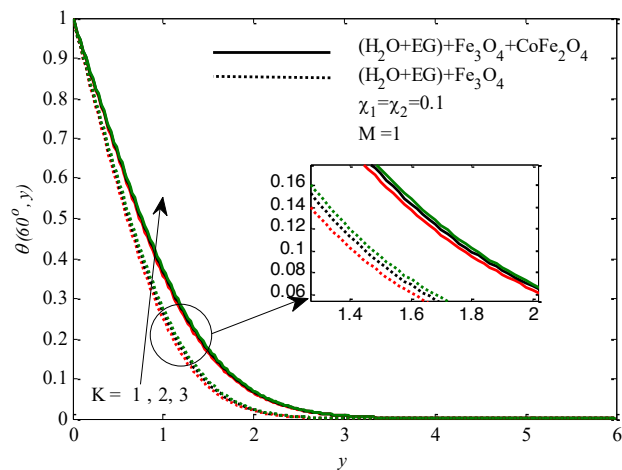


Fig. 10 Changes in θ due to variation in K

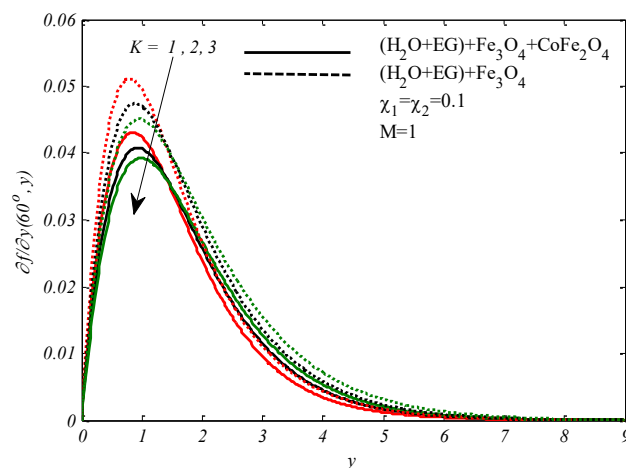


Fig. 11 Changes in $\partial f/\partial y$ due to variation in K

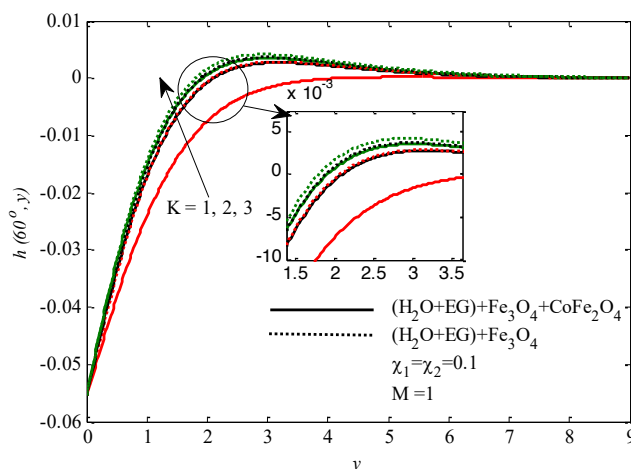


Fig. 12 Changes in θ due to variation in K

The effect of changing the micro-rotation parameter on the magnitude of the non-dimensional temperature profile in different y -positions at $x = 60^\circ$ is shown in Fig 10. As could be seen, for all vertical distances from the sphere surface the temperature is higher in the case of using hybrid instead of mono ferrofluid; also, the temperature is increased by increasing the micro-rotation parameter. The effect of altering K on the fluid temperature is not the same in all values of y and it works only near the sphere surface in the thermal boundary layer region. At $y = 0.6$, by increasing the value of K from 1 to 3, the non-dimensional temperature increased from 0.18 to 0.22 and from 0.35 to 0.4 in cases of using mono and hybrid ferrofluid. The increasing effect of using hybrid ferrofluid and increasing K value on temperature

The effect of employing different K values on velocity profile in cases of using mono and hybrid ferrofluid is shown in Fig. 11. As seen, different values of micro rotation parameters show their effect in most vicinity of the sphere surface ($y < 1.5$). In this region decreasing K would supers the velocity. After this point, the velocity profile increases when the values of K increases. This is due to the higher viscosity of mono ferrofluid than hybrid ferrofluid which would eventually give rise to boundary layer growth in this case. The variation of angular velocity vs for different K values in cases of using mono and hybrid ferrofluid is depicted in Fig. 12. By comparing Fig. 11 and Fig. 12 a different trend between the variations of velocity and angular velocity could be seen and, in each case, the angular velocity decreases through the way from the sphere surface. The separation point and the resulted reverse flow are observed for values K which take place near the vicinity of the

sphere surface. The higher reducing effect of mono ferrofluid than hybrid ferrofluid.

5. CONCLUSIONS

In this work, the impact of magnetic parameter, and micro-rotation on physical quantities heat transfer-related were numerically examined to achieve a comprehensive view of the heat transfer characteristics (water-ethylene glycol) 50% based micropolar hybrid ferrofluid flowing around a sphere, taking into account the combined convection and magnetic force. The following meaningful remarks deserve mention:

- All the physical quantities (C_f , Nu), velocity and angular velocity profiles which are studied in this work showed decreasing behavior when the values of magnetic parameter M increased. But the temperature profiles possess a proportional relationship with M .
- By increasing the K value, the temperature profiles, angular velocity profiles and local skin friction increased, but it opposite happens for the values of local Nusselt number values and velocity profiles.
- Whatever the values of parameters examined in this article, mono ferrofluid has the highest skin friction, heat transmission rate, and velocity and angular velocity profiles. Moreover, it has the lowest temperature

ACKNOWLEDGEMENTS

This publication was supported by the Deanship of Scientific Research at Ajloun National University, Ajloun 26810.

NOMENCLATURE

$C_{p,hff}$	Hybrid Ferrofluids heat capacity
g	Acceleration due to gravity
Gr	Grashof number
Γ	Micro-inertia density
K	Micro-rotation parameter
k_f	Base fluid thermal conductivity
k_s	Solid particles thermal conductivity
k_{hff}	Hybrid Ferrofluids thermal conductivity
\hat{H}	Angular velocity
Pr	Prandtl number
T	Temperature of the fluid
T_w	Wall temperature
T_∞	Ambient temperature
\hat{u}	\hat{x} -component of velocity
\hat{v}	\hat{y} -component of velocity

Greek Symbols

χ	Nanoparticles volume fraction
κ_0	Vortex viscosity
μ_f	Base fluid dynamic viscosity
μ_{hff}	Hybrid Ferrofluids dynamic viscosity
ρ_f	Base fluid density
ρ_s	Solid particles density
ρ_{hff}	Hybrid Ferrofluids density

β_f	Base fluid thermal expansion coefficient
β_s	Solid particles thermal expansion coefficient
γ_{hff}	Spin gradient viscosity
ϖ	Stream function
θ	Dimensionless temperature
<i>Subscripts</i>	
f	Base fluid
s	Solid particles
hff	Hybrid Ferrofluids
w	Condition at wall
∞	Condition at infinity

REFERENCES

- Abadeh, A., Mohammadi, M. and Passandideh-Fard, M., 2019. "Experimental investigation on heat transfer enhancement for a ferrofluid in a helically coiled pipe under constant magnetic field." *Journal of Thermal Analysis and Calorimetry*, **135**(2): 1069-1079. <https://doi.org/10.1007/s10973-018-7478-2>
- Abadeh, A., Sardarabadi, M., Abedi, M., Pourramezan, M., Passandideh-Fard, M. and Maghrebi, M. J., 2020. "Experimental characterization of magnetic field effects on heat transfer coefficient and pressure drop for a ferrofluid flow in a circular tube." *Journal of Molecular Liquids*, **299**: 112206. <https://doi.org/10.1016/j.molliq.2019.112206>
- Afzal, S., Siddique, I., Jarad, F., Ali, R., Abdal, S. and Hussain, S., 2021. "Significance of double diffusion for unsteady carreau micropolar nanofluid transportation across an extending sheet with thermo-radiation and uniform heat source." *Case Studies in Thermal Engineering*, **28**: 101397. <https://doi.org/10.1016/j.csite.2021.101397>
- Ahmadi, M. H., Mirlahi, A., Nazari, M. A. and Ghasempour, R., 2018. "A review of thermal conductivity of various nanofluids." *Journal of Molecular Liquids*, **265**: 181-188. <https://doi.org/10.1016/j.molliq.2018.05.124>
- Ajith, K., Pillai, A. S., Enoch, I. M. V., Sharifpur, M., Solomon, A. B. and Meyer, J., 2021. "Effect of the non-electrically conductive spindle on the viscosity measurements of nanofluids subjected to the magnetic field." *Colloids and Surfaces A: Physicochemical and Engineering Aspects*, **628**: 127252. <https://doi.org/10.1016/j.colsurfa.2021.127252>
- Al-Khaled, K., Khan, M. I., Khan, S. U., Malik, M. and Qayyum, S., 2021. "Non-uniform heat source/sink applications for the radiative flow of Brinkman micropolar nanofluid with microorganisms." *Computational and Theoretical Chemistry*, **1203**: 113330. <https://doi.org/10.1016/j.comptc.2021.113330>
- Alkasasbeh, H., 2018. "Numerical solution on heat transfer magnetohydrodynamic flow of micropolar Casson fluid over a horizontal circular cylinder with thermal radiation." *Frontiers in Heat and Mass Transfer (FHMT)*, **10**. <http://dx.doi.org/10.5098/hmt.10.32>
- Alkasasbeh, H., Swalmeh, M., Bani Saeed, H., Al Faqih, F. and Talafha, A., 2020. "Investigation on CNTs-water and human blood based Casson nanofluid flow over a stretching sheet under impact of magnetic field." *Frontiers in Heat and Mass Transfer (FHMT)*, **14**. <http://dx.doi.org/10.5098/hmt.14.15>
- Cebeci, T. and Bradshaw, P., 2012. *Physical and computational aspects of convective heat transfer*, Springer Science & Business Media.
- Chu, Y. M., Bilal, S. and Hajizadeh, M. R., 2020. "Hybrid ferrofluid along with MWCNT for augmentation of thermal behavior of fluid

during natural convection in a cavity.” *Mathematical Methods in the Applied Sciences*. <https://doi.org/10.1002/mma.6937>

El-dawy, H. and Gorla, R. S. R., 2021. “The flow of a micropolar nanofluid past a stretched and shrinking wedge surface with absorption.” *Case Studies in Thermal Engineering*, **26**: 101005. <https://doi.org/10.1016/j.csite.2021.101005>

Esfahani, J. A., Safaei, M. R., Goharimanesh, M., De Oliveira, L. R., Goodarzi, M., Shamshirband, S. and Bandarrah Filho, E. P., 2017. “Comparison of experimental data, modelling and non-linear regression on transport properties of mineral oil based nanofluids.” *Powder Technology*, **317**: 458-470. <https://doi.org/10.1016/j.powtec.2017.04.034>

García-Ortiz, J. H. and Galindo-Rosales, F. J., 2020. “Extensional Magnetorheology as a Tool for Optimizing the Formulation of Ferrofluids in Oil-Spill Clean-Up Processes.” *Processes*, **8**(5): 597. <https://doi.org/10.3390/pr8050597>

Giwa, S., Sharifpur, M., Goodarzi, M., Alsulami, H. and Meyer, J., 2021. “Influence of base fluid, temperature, and concentration on the thermophysical properties of hybrid nanofluids of alumina–ferrofluid: experimental data, modeling through enhanced ANN, ANFIS, and curve fitting.” *Journal of Thermal Analysis and Calorimetry*, **143**(6): 4149-4167. <https://doi.org/10.1007/s10973-020-09372-w>

Giwa, S., Sharifpur, M. and Meyer, J., 2020. “Effects of uniform magnetic induction on heat transfer performance of aqueous hybrid ferrofluid in a rectangular cavity.” *Applied Thermal Engineering*, **170**: 115004. <https://doi.org/10.1016/j.applthermaleng.2020.115004>

Gui, N. G. J., Stanley, C., Nguyen, N.-T. and Rosengarten, G., 2018. “Ferrofluids for heat transfer enhancement under an external magnetic field.” *International Journal of Heat and Mass Transfer*, **123**: 110-121. <https://doi.org/10.1016/j.ijheatmasstransfer.2018.02.100>

Habib, D., Abdal, S., Ali, R., Baleanu, D. and Siddique, I., 2021a. “On bioconvection and mass transpiration of micropolar nanofluid dynamics due to an extending surface in existence of thermal radiations.” *Case Studies in Thermal Engineering*, **27**: 101239. <https://doi.org/10.1016/j.csite.2021.101239>

Habib, U., Abdal, S., Siddique, I. and Ali, R., 2021b. “A comparative study on micropolar, Williamson, Maxwell nanofluids flow due to a stretching surface in the presence of bioconvection, double diffusion and activation energy.” *International Communications in Heat and Mass Transfer*, **127**: 105551. <https://doi.org/10.1016/j.icheatmasstransfer.2021.105551>

Hosseinzadeh, S. E., Majidi, S., Goharkhah, M. and Jahangiri, A., 2021. “Energy and exergy analysis of ferrofluid flow in a triple tube heat exchanger under the influence of an external magnetic field.” *Thermal Science and Engineering Progress*, **25**: 101019. <https://doi.org/10.1016/j.tsep.2021.101019>

Hosseinzadeh, K., Roghani, S., Asadi, A., Mogharrebi, A. and Ganji, D., 2020. “Investigation of micropolar hybrid ferrofluid flow over a vertical plate by considering various base fluid and nanoparticle shape factor.” *International Journal of Numerical Methods for Heat & Fluid Flow*. <https://doi.org/10.1108/HFF-02-2020-0095>

Huang, M. and Chen, G., 1987. “Laminar free convection from a sphere with blowing and suction.” *Journal of Heat Transfer (Transactions of the ASME (American Society of Mechanical Engineers), Series C; (United States))*, **109**(2). <https://doi.org/10.1115/1.3248117>

Hussain, S., Öztöp, H. F., Qureshi, M. A. and Abu-Hamdeh, N., 2020. “Magnetohydrodynamic flow and heat transfer of ferrofluid in a channel with non-symmetric cavities.” *Journal of Thermal Analysis and Calorimetry*, **140**(2): 811-823. <https://doi.org/10.1007/s10973-019-08943-w>

Jones, E., 1981. “An asymptotic outer solution applied to the Keller box method.” *Journal of Computational Physics*, **40**(2): 411-429. [https://doi.org/10.1016/0021-9991\(81\)90219-9](https://doi.org/10.1016/0021-9991(81)90219-9)

Kandelousi, M. S., 2017. *Nanofluid Heat and Mass Transfer in Engineering Problems*, BoD–Books on Demand. <http://dx.doi.org/10.5772/62719>

Karvelas, E., Sofiadis, G., Papatheanasiou, T. and Sarris, I., 2020. “Effect of micropolar fluid properties on the blood flow in a human carotid model.” *Fluids*, **5**(3): 125. <https://doi.org/10.3390/fluids5030125>

Keller, H. B. and Bramble, J., 1970. “Numerical solutions of partial differential equations.” *Mathematics*, **1**: 81-94.

Khan, A., Saeed, A., Tassaddiq, A., Gul, T., Mukhtar, S., Kumam, P., Ali, I. and Kumam, W., 2021a. “Bio-convective micropolar nanofluid flow over thin moving needle subject to Arrhenius activation energy, viscous dissipation and binary chemical reaction.” *Case Studies in Thermal Engineering*, **25**: 100989. <https://doi.org/10.1016/j.csite.2021.100989>

Khan, M. I., Al-Khaled, K., Khan, S. U., Muhammad, T., Waqas, H., El-Refaey, A. M. and Khan, M. I., 2021b. “Dynamic consequences of nonlinear radiative heat flux and heat generation/absorption effects in cross-diffusion flow of generalized micropolar nanofluid.” *Case Studies in Thermal Engineering*, **28**: 101451. <https://doi.org/10.1016/j.csite.2021.101451>

Kole, M. and Khandekar, S., 2021. “Engineering applications of ferrofluids: A review.” *Journal of Magnetism and Magnetic Materials*: 168222. <https://doi.org/10.1016/j.jmmm.2021.168222>

Kumar, K. A., Sandeep, N., Sugunamma, V. and Animesaun, I., 2020. “Effect of irregular heat source/sink on the radiative thin film flow of MHD hybrid ferrofluid.” *Journal of Thermal Analysis and Calorimetry*, **139**(3): 2145-2153. <https://doi.org/10.1007/s10973-019-08628-4>

Li, Z., Li, D. and Chen, Y., 2020. “Study on the yielding behaviors of ferrofluids: a very shear thinning phenomenon.” *Soft Matter*, **16**(35): 8202-8212. <https://doi.org/10.1039/D0SM00778A>

Mahian, O., Bellos, E., Markides, C. N., Taylor, R. A., Alagumalai, A., Yang, L., Qin, C., Lee, B. J., Ahmadi, G. and Safaei, M. R., 2021. “Recent advances in using nanofluids in renewable energy systems and the environmental implications of their uptake.” *Nano Energy*: 106069. <http://dx.doi.org/10.1016/j.nanoen.2021.106069>

Mehrez, Z. and El Cafi, A., 2021. “Heat exchange enhancement of ferrofluid flow into rectangular channel in the presence of a magnetic field.” *Applied Mathematics and Computation*, **391**: 125634. <https://doi.org/10.1016/j.amc.2020.125634>

Moghadam, H. K., Baghbani, S. S. and Babazadeh, H., 2021. “Study of thermal performance of a ferrofluid with multivariable dependence viscosity within a wavy duct with external magnetic force.” *Journal of Thermal Analysis and Calorimetry*, **143**(5): 3849-3866. <https://doi.org/10.1007/s10973-020-09324-4>

Mohamed, M. K. A., Yasin, S. H. M., Salleh, M. Z. and Alkasasbeh, H. T., 2021. “MHD Stagnation Point Flow and Heat Transfer Over a Stretching Sheet in a Blood-Based Casson Ferrofluid With Newtonian Heating.” *Journal of Advanced Research in Fluid Mechanics and Thermal Sciences*, **82**(1): 1-11. <https://doi.org/10.37934/arfm.82.1.111>

Patra, J. K., Das, G., Fraceto, L. F., Campos, E. V. R., del Pilar Rodriguez-Torres, M., Acosta-Torres, L. S., Diaz-Torres, L. A., Grillo, R., Swamy, M. K. and Sharma, S., 2018. “Nano based drug delivery systems: recent developments and future prospects.” *Journal of nanobiotechnology*, **16**(1): 1-33. <https://doi.org/10.1186/s12951-018-0392-8>

Ramesh, G., Roopa, G., Rauf, A., Shehzad, S. and Abbasi, F., 2021. "Time-dependent squeezing flow of Casson-micropolar nanofluid with injection/suction and slip effects." *International Communications in Heat and Mass Transfer*, **126**: 105470.

<https://doi.org/10.1016/j.icheatmasstransfer.2021.105470>

Saeedi, A. H., Akbari, M. and Toghraie, D., 2018. "An experimental study on rheological behavior of a nanofluid containing oxide nanoparticle and proposing a new correlation." *Physica E: Low-Dimensional Systems and Nanostructures*, **99**: 285-293.

<https://doi.org/10.1016/j.physe.2018.02.018>

Saikrishnan, P., Jenifer, A. S., and Rajakumar, J., 2021. Steady MHD flow over a yawed cylinder with mass transfer. *Frontiers in Heat and Mass Transfer (FHMT)*, **17**: 1-8. <http://dx.doi.org/10.5098/hmt.17.4>

Sahim, K., Puspitasari, D., and Nukman, N., 2021. "Experimental study of convective heat transfer of alumina oxide nanofluids in triangle channel with uniform heat flux." *Frontiers in Heat and Mass Transfer (FHMT)*, **16**: 1-6 <http://dx.doi.org/10.5098/hmt.16.22>

Swalmeh, M. Z., Alkasasbeh, H. T., Hussanan, A. and Mamat, M., 2018. "Heat transfer flow of Cu-water and Al₂O₃-water micropolar nanofluids about a solid sphere in the presence of natural convection using Keller-box method." *Results in Physics*, **9**: 717-724.

<https://doi.org/10.1016/j.rinp.2018.03.033>

Tadesse, F. B., Makinde, O. D. and Enyadene, L. G., 2021. "Hydromagnetic stagnation point flow of a magnetite ferrofluid past a

convectively heated permeable stretching/shrinking sheet in a Darcy–Forchheimer porous medium." *Sādhanā*, **46**(3): 1-17.

<https://doi.org/10.1007/s12046-021-01643-y>

Tlili, I., Mustafa, M., Kumar, K. A. and Sandeep, N., 2020. "Effect of asymmetrical heat rise/fall on the film flow of magnetohydrodynamic hybrid ferrofluid." *Scientific reports*, **10**(1): 1-11.

<https://doi.org/10.1038/s41598-020-63708-y>

Toghraie, D. S., Sina, N., Mozafarifar, M., Alizadeh, A. a., Soltani, F. and Fazilati, M. A., 2020. "Prediction of dynamic viscosity of a new non-Newtonian hybrid nanofluid using experimental and artificial neural network (ANN) methods." *Heat Transfer Research*, **51**(15).

<https://doi.org/10.1615/heattransres.2020034645>

Wang, E. C. and Wang, A. Z., 2014. "Nanoparticles and their applications in cell and molecular biology." *Integrative biology*, **6**(1): 9-26. <https://doi.org/10.1039/c3ib40165k>

Waqas, H., Alqarni, M., Muhammad, T. and Khan, M. A., 2021. "Numerical study for bioconvection transport of micropolar nanofluid over a thin needle with thermal and exponential space-based heat source." *Case Studies in Thermal Engineering*: 101158.

<https://doi.org/10.1016/j.csite.2021.101158>

Zheng, D., Yang, J., Wang, J., Kabelac, S. and Sundén, B., 2021. "Analyses of thermal performance and pressure drop in a plate heat exchanger filled with ferrofluids under a magnetic field." *Fuel*, **293**: 120432.

<https://doi.org/10.1016/j.fuel.2021.120432>